energies

MDPI

Article

Triple Line-Voltage Cascaded VIENNA Converter Applied as the Medium-Voltage AC Drive

Jia Zou *, Cong Wang, Hong Cheng and Jinqi Liu

Department of Information and Electrical Engineering, China University of Mining & Technology (Beijing), Beijing 100083, China; wangc@cumtb.edu.cn (C.W.); chengh@cumtb.edu.cn (H.C.); 15333003179@163.com (J.L.)
* Correspondence: zjia@cumtb.edu.cn or zoujia007@126.com; Tel.: +86-136-8367-7117

Received: 5 April 2018; Accepted: 24 April 2018; Published: 27 April 2018

Abstract: A novel rectifier based on a triple line-voltage cascaded VIENNA converter (LVC-VC) was proposed. Compared to the conventional cascaded H-bridge converters, the switch voltage stress is lower, and the numbers of switches and dc capacitors are fewer under similar operating conditions in the proposed new multilevel converter. The modeling and control for the LVC-VC ware presented. Based on the analysis of the operation principle of the new converter, the power factor correction of the proposed converter was realized by employing a traditional one-cycle control strategy. The minimum average value and maximum harmonic components of the dc-link voltages of the three VIENNA rectifier modules ware calculated. Three VIENNA dc-link voltages were unbalanced under the unbalanced load conditions, so the zero sequence current was injected to the three inner currents for balancing three VIENNA dc-link voltages. Simulation and the results of the experiment verified the availability of the new proposed multilevel converter and the effectiveness of the corresponding control strategy applied.

Keywords: line voltage cascaded VIENNA converter (LVC-VC); power factor correction (PFC); one-cycle control (OCC); zero-sequence current injection

1. Introduction

Recently, owing to the particular characteristics of withstanding a high voltage and generating nearly sinusoidal waveforms with low electromagnetic interference, a reduced common-mode voltage, and a high efficiency, the "multilevel converters" have aroused strong attention in the power electronics research field [1], and are extremely hopeful for power system applications such as power electronic transformers, static VAR generators, high power high voltage adjustable AC speed drives, etc. The neutral-point clamped converter (NPC) [2], flying capacitor converter (FC), and cascaded H-bridge converter (CHB) [3] are the most common multilevel converter topologies. The products based on NPC typology developed by ABB and Siemens and those based on CHB typology developed by Robicon Corp. have become increasingly popular in high power medium-voltage AC drive applications. However, the primary disadvantage of the two kinds of products is that they both require a bulky and expensive multi-winding line-frequency transformer in the rectifier stage, and the transformer's weight and cost occupy a very large ratio of the convert.

In the past decades, the multilevel converter based on the high frequency transformer has rapidly developed [4–7], and by using a cascaded H-bridge converter (CHB), it could achieve direct connection to the high voltage power grid. What is more, the use of CHB generates many extra advantageous characteristics, such as better power quality and flexible control of the output voltage [8]. The primary disadvantage of this kind of multilevel converter is that numerous fully-controlled semiconductor devices and dc capacitances are required [9], thus increasing the system control complexity and costs.

To resolve the aforementioned shortcomings, a three-phase-bridge cascaded converter has been proposed [10–17]. There are fewer switches and dc capacitors in this kind of converter. Enlightened by the above-mentioned converters, and considering that, in practice, in a lot of industrial applications, the bi-directional power flow is not necessarily required, such as in speed regulation with pumps or fans load, this paper proposes a new topology of a unidirectional multilevel converter based on line-voltage cascaded three-phase-VIENNA converters (LVC-VC). Compared to conventional three-phase CHB converters, in the proposed new multilevel converters, the switch voltage stress is much lower, and fewer power switches and dc capacitors are required under similar operation conditions, as is shown in Table 1. From the overall loss analysis, the total losses consist of two parts: conduction and switching losses [18]. Regarding the total of IGBT and diode losses, because the numbers of switches and dc capacitors are fewer and the high voltage diode conduction losses are very few, the conduction losses of the proposed converter are less than the cascaded H-bridge converter.

Table 1. The comparison of three-phase CHB and LVC-VC.

Line-Line Voltage 6000 V (rsm) Convert	Cascaded Series	The Approximate Value of dc-Link Voltages of Each Cascaded Converter	The Switch Stress	The Number of Switches	The Number of dc Capacitors	The Diode Number
Three phase cascaded H-bridge converter (CHB)	3	2.3 KV	2.3 KV	36	9	0
Triple Line-Voltage Cascaded VIENNA Converter	2	4.8 KV	2.4 KV	9	6	18

Figure 1 shows a possible topology of a high-voltage power system with the new proposed multilevel converter (LVC-VC) as the rectifier stage. The line-frequency transformer is eliminated in this power conversion system by utilization of the high frequency dc/dc converters in the middle stage. The inverter stage is similar to that of the ABB MV Drives ACS5000.

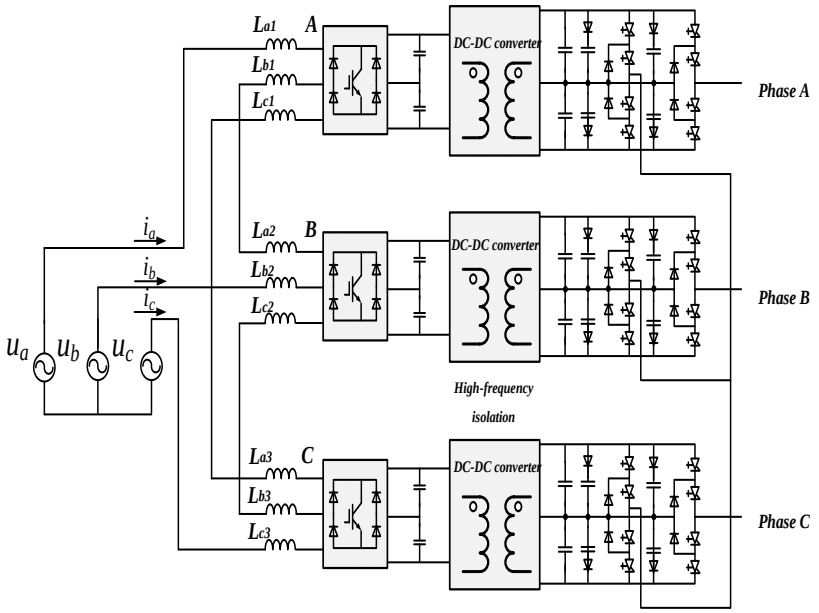

Figure 1. New topology of the medium voltage power converter.

The paper is divided into five sections. Section 2 states the theories of the suggested triple LVC-VC, including the topology configuration and the steady-state mathematical models. Section 3 presents the PWM PFC strategy based on one-cycle control. In Section 4, a discussion on the dc link voltages of

three VIENNA rectifier modules is carried out. Section 5 presents a hierarchical control strategy to realize a desired power factor and the balanced output dc voltages. In order to balance the dc-link voltages of the three VIENNA converters, an injected zero sequence current control strategy is studied. The simulation and experiment are presented to confirm the effectiveness of the academic method.

2. Operation Principles of Triple LVC-VC

2.1. Circuit Configuration

The triple LVC-VC is operated in Figure 2a, and as shown, three VIENNA-rectifier modules bridges are interconnected in a line voltage series connection mode. u_a, u_b, u_c are three-phase power supply voltages; L_{ai}, L_{bi}, L_{ci} (i = 1, 2, 3) represent the ac-side filtering inductance of the three VIENNA rectifiers; u_{O1}, u_{O2}, u_{O3} are the three dc-link voltages; C_{x1}, C_{x2} ($x = a, b, c$) are the dc-link capacitances, assuming they are all have an equal value C; and R_1, R_2, R_3 are the loads of the three VIENNA rectifiers. Figure 2b shows the simplified connecting structure of LVC-VC.

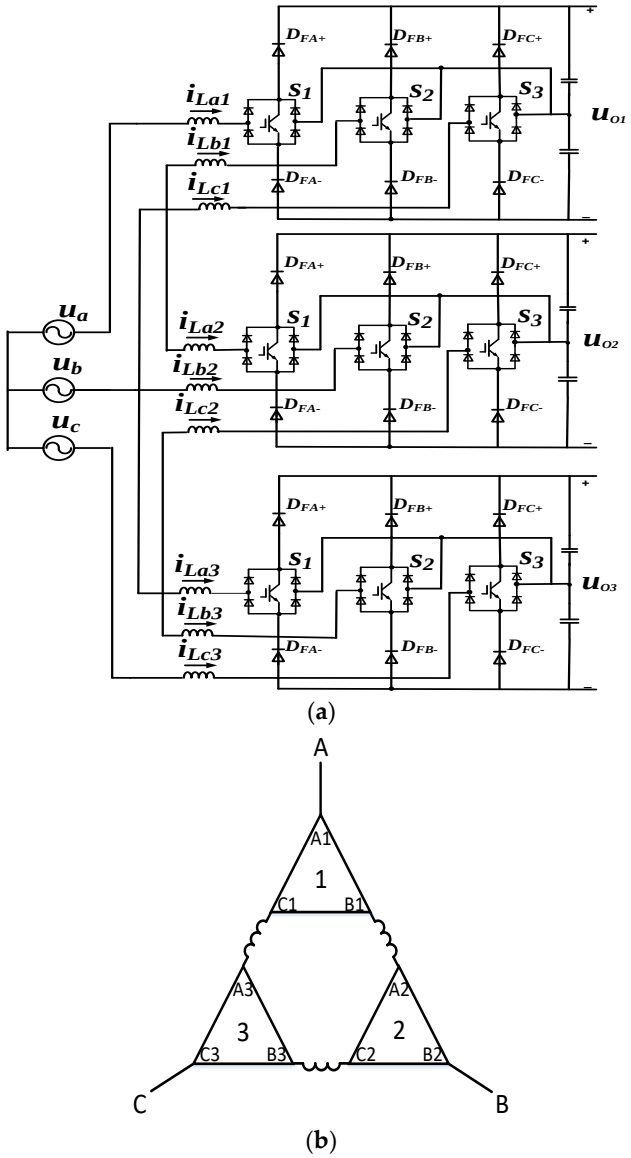

Figure 2. Triple line voltage cascaded VIENNA converter. (**a**) the schematic circuit diagram. (**b**) simplified connected structure diagram.

2.2. Analysis to Pole Voltages and Input Currents

Figure 3a shows the LVC-VC circuit with ideal bidirectional switches. This assumes that LVC-VC is connected to the balanced loads with equal dc-link voltages ($u_{O1} = u_{O2} = u_{O3}$), and the voltage fluctuation of the two split capacitors is negligible.

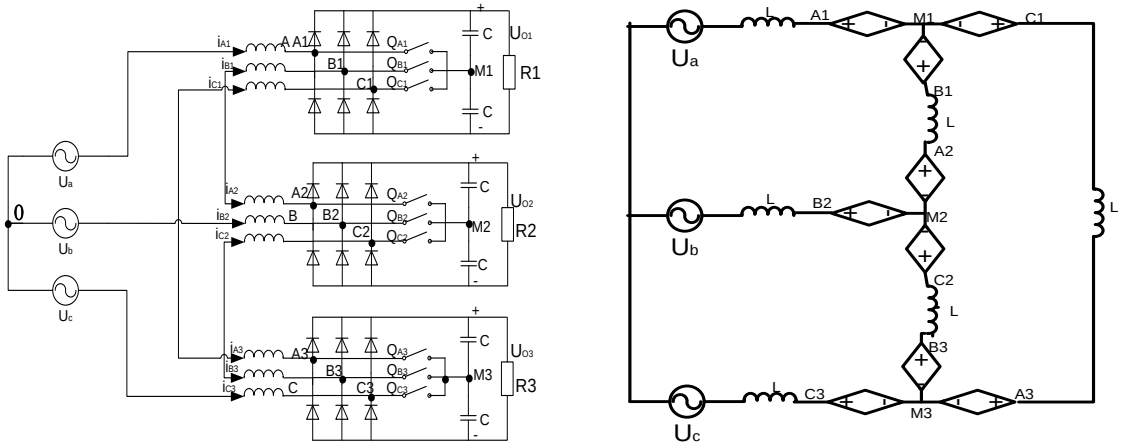

(**a**) (**b**)

Figure 3. (**a**) triple line voltage cascaded VIENNA rectifier. (**b**) the switching cycle average model of the converter.

According to the principle, the average voltages at nodes *Ai*, *Bi*, *Ci* (*i* = 1, 2, 3) referring to the common point of the two split capacitors of the three VIENNA converters as presented in Figure 3a are given by [19]:

$$\begin{cases} u_{A_iM_i} = \frac{u_O}{2}\mathrm{sgn}(i_{Ai})(1 - S_{Ai}) \\ u_{B_iM_i} = \frac{u_O}{2}\mathrm{sgn}(i_{Bi})(1 - S_{Bi}) \\ u_{C_iM_i} = \frac{u_O}{2}\mathrm{sgn}(i_{ci})(1 - S_{Ci}) \end{cases} \quad (1)$$

where $\mathrm{sgn}(x) = \begin{cases} -1, & x < 0 \\ 1, & x \geq 0 \end{cases}$, is the sign function; and S_{xi} (X = A, B, C, and i = 1, 2, 3) are the duty ratios of switches Q_{xi} (X = A, B, C, and i = 1, 2, 3).

Figure 3b describes the cycle average model of LVC-VC. When the converter is operating in such a way as $S_{B1} = S_{A2}$, $S_{C2} = S_{B3}$ and $S_{A3} = S_{C1}$, then there will be $u_{B_1M_1} = -u_{A_2M_2}$, $u_{C_2M_2} = -u_{B_3M_3}$, $u_{A_3M_3} = -u_{C_1M_1}$. Under such a condition, the input line currents can be expressed as:

$$\begin{cases} i_{A1} = \frac{1}{4}[3(u_a - u_{A1M1}) + 2(u_{B1M1} + u_{C1M1})]/SL \\ i_{B2} = \frac{1}{4}[3(u_b - u_{B2M2}) + 2(u_{C2M2} + u_{A2M2})]/SL \\ i_{C3} = \frac{1}{4}[3(u_c - u_{C3M3}) + 2(u_{A3M3} + u_{B3M3})]/SL \end{cases} \quad (2)$$

When $u_{A1M1}, u_{B2M2}, u_{C3M3}$ and $u_{B1M1}, u_{C2M2}, u_{A3M3}$ can be controlled symmetrically and sinusoidally, the fundamentals of three input currents provided by the power supply can be expressed as:

$$\begin{cases} i_A = i_{A1} = \sqrt{2}I\sin(\omega t) \\ i_B = i_{B2} = \sqrt{2}I\sin(\omega t - 120^\circ) \\ i_C = i_{C3} = \sqrt{2}I\sin(\omega t + 120^\circ) \end{cases} \quad (3)$$

If each VIENNA module is a generalized node, then the LVC-VC converter can be simplified further, and three VIENNA converter modules in Δ connection are Y-connected to the three-phase power supply. According to the relationship between line current and phase current, from Equation (3)

and Figure 3b, the fundamentals of three input currents for each VIENNA converter module can be obtained conveniently, as follows:

$$\begin{cases} i_{A1} = \sqrt{2} I \sin(\omega t) \\ i_{B1} = \sqrt{\frac{2}{3}} I \sin(\omega t - 150^\circ) \\ i_{C1} = \sqrt{\frac{2}{3}} I \sin(\omega t + 150^\circ) \end{cases} \tag{4}$$

$$\begin{cases} i_{A2} = \sqrt{\frac{2}{3}} I \sin(\omega t + 30^\circ) \\ i_{B2} = \sqrt{2} I \sin(\omega t - 120^\circ) \\ i_{C2} = \sqrt{\frac{2}{3}} I \sin(\omega t + 90^\circ) \end{cases} \tag{5}$$

$$\begin{cases} i_{A3} = \sqrt{\frac{2}{3}} I \sin(\omega t - 30^\circ) \\ i_{B3} = \sqrt{\frac{2}{3}} I \sin(\omega t - 90^\circ) \\ i_{C3} = \sqrt{2} I \sin(\omega t + 120^\circ) \end{cases} \tag{6}$$

Figure 4 shows the AC currents phasor diagram of the LVC-VC. The fundamentals of three input currents for each VIENNA converter module can be obtained conveniently with the help of Equations (4)–(6), where i_{A1} i_{B2} i_{C3} are three line currents and the others are the phase currents.

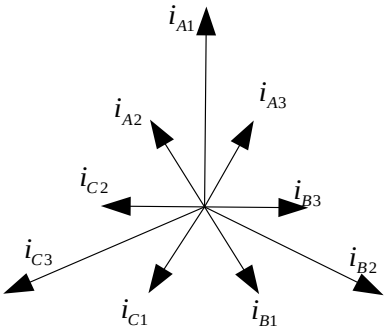

Figure 4. The AC currents phasor diagram of the LVC-VC.

3. PWM Strategy

As a high quality three-phase rectifier, three power phase currents should be sinusoidal and symmetrical.

3.1. The Equivalent Multilevel Series of the LVC-VC

With a combination of Figure 3b and Equation (2), a three-phase delta connected cascaded VIENNA rectifier could be equivalent to the three phase star-connected circuit in Figure 5.

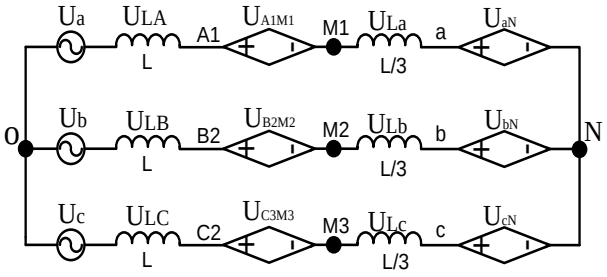

Figure 5. The equivalent star-connected circuit of three-phase delta connected LVC-VC.

In this circuit,

$$\begin{cases} U_{aN} = -\frac{2}{3}(U_{B1M1} + U_{C1M1}) \\ U_{bN} = -\frac{2}{3}(U_{C2M1} + U_{A2M2}) \\ U_{cN} = -\frac{2}{3}(U_{A3M3} + U_{B3M3}) \end{cases} \tag{7}$$

The inductor voltage can be ignored because of its small size compared to the line voltage. A combination of (1) and (7) yields the three bridge phase voltages, which can be expressed as:

$$u_{A1N} = \frac{u_O}{2}\left\{\mathrm{sgn}(i_{A1})(1 - S_{A1}) - \frac{2}{3}[\mathrm{sgn}(i_{B1})(1 - S_{B1}) + \mathrm{sgn}(i_{C1})(1 - S_{C1})]\right\} \tag{8}$$

Assuming $E = \frac{u_O}{2}$, there are 13 kinds of levels for the u_{A1N}, as the on or off of power switches and the ac current direction are different, as shown in Table 2.

Table 2. The convert equivalent multilevel series.

s_{A1}	s_{B1}	s_{C1}	i_{A1}	i_{B1}	i_{C1}	u_{A1M1}	u_{B1M1}	u_{C1M1}	u_{A1N}
1	1	1	/	/	/	0	0	0	0
0	0	1	+	+	−	E	E	0	1/3E
0	0	1	−	−	+	−E	−E	0	−1/3E
1	1	0	+	+	−	0	0	−E	2/3E
1	1	0	−	−	+	0	0	E	−2/3E
0	1	1	+	−	−	E	0	0	E
0	1	1	−	+	+	−E	0	0	−E
1	0	0	+	−	−	0	−E	−E	4/3E
1	0	0	−	+	+	0	E	E	−4/3E
0	0	1	+	−	−	E	−E	0	5/3E
0	0	1	−	+	+	−E	E	0	−5/3E
0	0	0	+	−	−	E	−E	−E	7/3E
0	0	0	−	+	+	−E	E	E	−7/3E

3.2. Three Phase Unity Power Factor

Although the basic working principle of a one-cycle control(OCC) based three phase VIENNA converter has been presented in several papers previously [19,20], for the sake of completeness, it is still briefly described in this paper. If we assume that the inductances for all three-phases are the same, the dynamics of three ac-side voltages of LVC-VC can be written as in [19].

$$\begin{bmatrix} \frac{2}{3} & -\frac{1}{3} & -\frac{1}{3} \\ -\frac{1}{3} & \frac{2}{3} & -\frac{1}{3} \\ -\frac{1}{3} & -\frac{1}{3} & \frac{2}{3} \end{bmatrix} \times \begin{bmatrix} U_{A1N} \\ U_{B2N} \\ U_{C3N} \end{bmatrix} = \begin{bmatrix} U_a \\ U_b \\ U_c \end{bmatrix} \tag{9}$$

The combination of (1) and (7) yields:

$$\begin{cases} U_{A1N} = \frac{U_0}{2}\left\{\mathrm{sgn}(i_{A1})(1 - S_{A1}) - \frac{2}{3}[\mathrm{sgn}(i_{B1})(1 - S_{B1}) + \mathrm{sgn}(i_{C1})(1 - S_{C1})]\right\} \\ U_{B2N} = \frac{U_0}{2}\left\{\mathrm{sgn}(i_{B2})(1 - S_{B2}) - \frac{2}{3}[\mathrm{sgn}(i_{C2})(1 - S_{C2}) + \mathrm{sgn}(i_{A2})(1 - S_{A2})]\right\} \\ U_{C3N} = \frac{U_0}{2}\left\{\mathrm{sgn}(i_{C3})(1 - S_{C3}) - \frac{2}{3}[\mathrm{sgn}(i_{A3})(1 - S_{A3}) + \mathrm{sgn}(i_{B3})(1 - S_{B3})]\right\} \end{cases} \tag{10}$$

Its control goal is given by:

$$\begin{cases} U_a = R_e \times i_{A1} \\ U_b = R_e \times i_{B2} \\ U_c = R_e \times i_{C3} \end{cases} \tag{11}$$

$$V_m = \frac{U_O \times R_s}{2 \times R_e} \tag{12}$$

where V_m is the dc-link voltage loop compensator.

From Equations (9)–(12), one simple solution can be found expressed as:

$$\begin{cases} V_m \times \mathrm{sgn}(i_{A1})(1 - S_{A1}) = K_1 \times i_{A1} \\ V_m \times \mathrm{sgn}(i_{B2})(1 - S_{B2}) = K_1 \times i_{B2} \\ V_m \times \mathrm{sgn}(i_{C3})(1 - S_{C3}) = K_1 \times i_{C3} \end{cases} \tag{13}$$

$$\begin{cases} V_m \times \mathrm{sgn}(i_{B1})(1 - S_{B1}) = K_2 \times i_{B1} \\ V_m \times \mathrm{sgn}(i_{C2})(1 - S_{C2}) = K_2 \times i_{C2} \\ V_m \times \mathrm{sgn}(i_{A3})(1 - S_{A3}) = K_2 \times i_{A3} \end{cases} \tag{14}$$

$$\begin{cases} V_m \times \mathrm{sgn}(i_{C1})(1 - S_{C1}) = K_2 \times i_{C1} \\ V_m \times \mathrm{sgn}(i_{A2})(1 - S_{A2}) = K_2 \times i_{A2} \\ V_m \times \mathrm{sgn}(i_{B3})(1 - S_{B3}) = K_2 \times i_{B3} \end{cases} \tag{15}$$

where, K_2, K_4 are constant, it can be determined by:

$$\begin{bmatrix} \frac{2}{3} & -\frac{1}{3} & -\frac{1}{3} \\ -\frac{1}{3} & \frac{2}{3} & -\frac{1}{3} \\ -\frac{1}{3} & -\frac{1}{3} & \frac{2}{3} \end{bmatrix} \times \left\{ K_2 \begin{bmatrix} i_{A1} \\ i_{B2} \\ i_{C3} \end{bmatrix} - \frac{2}{3} K_2 \begin{bmatrix} i_{B1}+i_{C1} \\ i_{C2}+i_{A2} \\ i_{A3}+i_{B3} \end{bmatrix} \right\} = R_s \begin{bmatrix} i_{A1} \\ i_{B2} \\ i_{C3} \end{bmatrix} \tag{16}$$

where, $i_{A1} + i_{B1} + i_{C1} = i_{A2} + i_{B2} + i_{C2} = i_{A3} + i_{B3} + i_{C3} = 0$.

This yields:

$$K_1 + K_2 \times \frac{2}{3} = R_s \tag{17}$$

Assume, $K_2 = K_1 \times \sqrt{3}$. Equations (13)–(15) can be expressed as:

$$\begin{cases} V_m \times (1 - S_{A1}) = K_1 \times |i_{A1}| \\ V_m \times (1 - S_{B2}) = K_1 \times |i_{B2}| \\ V_m \times (1 - S_{C3}) = K_1 \times |i_{C3}| \end{cases} \tag{18}$$

$$\begin{cases} V_m \times (1 - S_{B1}) = \sqrt{3} \times K_1 \times |i_{B1}| \\ V_m \times (1 - S_{C2}) = \sqrt{3} \times K_1 \times |i_{C2}| \\ V_m \times (1 - S_{A3}) = \sqrt{3} \times K_1 \times |i_{A3}| \end{cases} \tag{19}$$

$$\begin{cases} V_m \times (1 - S_{C1}) = \sqrt{3} \times K_1 \times |i_{C1}| \\ V_m \times (1 - S_{A2}) = \sqrt{3} \times K_1 \times |i_{A2}| \\ V_m \times (1 - S_{B3}) = \sqrt{3} \times K_1 \times |i_{B3}| \end{cases} \tag{20}$$

Those are the control key equations for the triple LVC-VC.

3.3. Currents Control by One-Cycle Control

The one-cycle control strategy has been previously discussed in much literature. Equations (21)–(23) give the key control equation for the one-cycle control strategy. Figure 6 shows the control block in view of the one-cycle control algorithm. The control system is composed of a voltage compensator and the OCC controller. In the voltage compensator, the error between the reference voltage and sensed dc-link voltage is adjusted by a PI controller, and the output signal V_m is considered as the input of a carrier generator. The output of the carrier generator is connected to the input of a comparator, and the triangular waveforms synthesized by the carrier generator are compared with the sampled input currents. Then, 9 pwm signals are generated to control the on and off state of the nine switches in the three VIENNA converter modules, and force the average inductor currents over one switching cycle in each of the VIENNA modules to follow the corresponding phase voltages. In order

to increase the utilization of the carrier wave, the magnitude of the triangular waveforms compared with the three-line currents is set to be $\sqrt{3}$ times that of the other six phase currents.

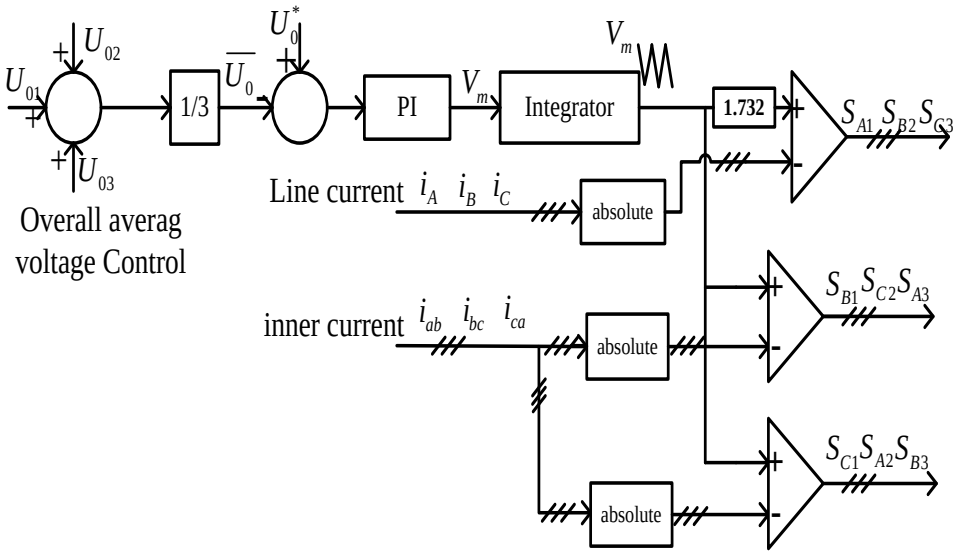

Figure 6. The one-cycle control block.

4. Analysis to the dc-Link Voltages of Triple LVC-VC

The voltage stress for each power switch in the proposed Triple LVC-VC directly depends on the value of the dc-link voltage of each module.

4.1. Three dc-Link Voltages of Triple LVS-VC

From Figure 3a, the dynamics of the three dc-link voltages of LVC-VC can be written in the abc stationery frame as in [21].

$$\begin{cases} C\frac{du_{o1}}{dt} = d_{A1}i_{A1} + d_{B1}i_{B1} + d_{C1}i_{C1} - 2\frac{u_{o1}}{R_1} \\ C\frac{du_{o2}}{dt} = d_{A2}i_{A2} + d_{B2}i_{B2} + d_{C2}i_{C2} - 2\frac{u_{o2}}{R_2} \\ C\frac{du_{o3}}{dt} = d_{A3}i_{A3} + d_{B3}i_{B3} + d_{C3}i_{C3} - 2\frac{u_{o3}}{R_3} \end{cases} \tag{21}$$

where, d_{Ai}, d_{Bi}, d_{Ci} are the fundamental components of switching functions of voltages $u_{X_iM_i}$.

From Equations (13)–(15) and (18)–(20), the following dynamics can be written:

$$\begin{cases} d_{A1} = \mathrm{sgn}(i_{A1})(1 - S_{A1}) = M\sin(\omega t) \\ d_{B1} = \mathrm{sgn}(i_{B1})(1 - S_{B1}) = M\sin(\omega t - 150^\circ) \\ d_{C1} = \mathrm{sgn}(i_{C1})(1 - S_{C1}) = M\sin(\omega t + 150^\circ) \end{cases} \tag{22}$$

$$\begin{cases} d_{A2} = \mathrm{sgn}(i_{A2})(1 - S_{A2}) = M\sin(\omega t + 30^\circ) \\ d_{B2} = \mathrm{sgn}(i_{B2})(1 - S_{B2}) = M\sin(\omega t - 120^\circ) \\ d_{C2} = \mathrm{sgn}(i_{C2})(1 - S_{C2}) = M\sin(\omega t + 90^\circ) \end{cases} \tag{23}$$

$$\begin{cases} d_{A3} = \mathrm{sgn}(i_{A3})(1 - S_{A3}) = M\sin(\omega t - 30^\circ) \\ d_{B3} = \mathrm{sgn}(i_{B3})(1 - S_{B3}) = M\sin(\omega t - 90^\circ) \\ d_{C3} = \mathrm{sgn}(i_{C3})(1 - S_{C3}) = M\sin(\omega t + 120^\circ) \end{cases} \tag{24}$$

where M is the modulation ratio for the three switches connected to the power line and the other six inner switches in the Triple LVC-VC.

From Equations (21)–(24), the dc-link voltages for each VIENNA module can be obtained as:

$$\begin{cases} u_{o1} = \frac{K_3}{2} IR_1 - \frac{K_4}{2} \frac{IR_1}{\sqrt{C^2R^2\omega^2+1}} \sin(2\omega t) \\ u_{o2} = \frac{K_3}{2} IR_2 - \frac{K_4}{2} \frac{IR_2}{\sqrt{C^2R^2\omega^2+1}} \sin(2\omega t + 120^\circ) \\ u_{o3} = \frac{K_3}{2} IR_3 - \frac{K_4}{2} \frac{IR_3}{\sqrt{C^2R^2\omega^2+1}} \sin(2\omega t + 240^\circ) \end{cases} \quad (25)$$

where $K_3 = \left(\frac{\sqrt{2}}{2} + \sqrt{\frac{2}{3}} \right) M$, $K_4 = (\frac{\sqrt{2}}{2} + \sqrt{\frac{1}{6}}) M$.

Equation (25) indicates that each dc-link voltage is composed of two parts, where the first part represents the direct current component of the dc-link voltage or the average value of u_{oi}, and the other one with a double fundamental frequency stands for the ac component of dc-link voltages.

4.2. The Maximum AC Component of dc-Link Voltages

Equation (25) shows that a double fundamental frequency component $\widetilde{u_{oi}}$ is superimposed *on* u_{oi}. The magnitude of the ac component $\widetilde{u_{oi}}$ can be expressed by Equation (11) as:

$$\widetilde{u_o} = \frac{K_4}{2} \frac{IR}{\sqrt{C^2R^2\omega^2+1}} \approx \frac{K_4}{2} \frac{I}{\omega C} \quad (26)$$

Making M in Equation (26) equal to 1, the maximum magnitude of ac component can be written as:

$$\widetilde{u_{o}}_{max} \approx 0.56 \frac{I}{\omega C} \quad (27)$$

Since the ac component is not very big, it may only slightly influence the fluctuation.

4.3. The Minimum dc-Link Average Voltages

Three loads of the three VIENNA rectifiers are similar, $R_1 = R_2 = R_3 = R$. From Equation (25), the dc component can be written as:

$$\overline{u_o} = \frac{K_3}{2} IR \quad (28)$$

Considering the power balance, the following equation should be satisfied:

$$P = \frac{u_{o1}^2}{R} + \frac{u_{o2}^2}{R} + \frac{u_{o3}^2}{R} = \sqrt{3}UI \quad (29)$$

here, U and I are AC effective values of power supply.

The following equation is obtained from Equations (28) and (29):

$$\overline{u_o} = \frac{2U}{\sqrt{3} \times K_3} \quad (30)$$

When M is set to be 1, the lowest value of the dc-link voltage required by each module of the converter can be written as:

$$\overline{u_o}_{min} \approx 0.76U \quad (31)$$

Equation (31) shows that the voltage stress of power switches in the proposed LVC-VC is much more reduced. For example, when the LVC-VC converter is connected to the power supply with the 6 KV line-line voltage, the average dc-link voltage of every VIENNA converter module can be set to 4.8 KV. In this case, the voltage stress of each switch is only 2.4 KV, which is 50 percent of the dc-link voltage, so the power switch with a much lower voltage rating can be employed in the converter.

5. System Controller Design

The controller design in the following should include two things: (1) Making the LVC-VC always operate under a unity power factor; (2) making the dc-link voltages of the three VIENNA converter modules always keep balance with either balanced loads or unbalanced loads.

5.1. Balancing Control to the Three dc-Link Voltages of VIENNA Rectifier

When the loads connected to the three VIENNA modules are different, imbalance will occur in the three dc-link voltages. With the goal of maintaining the balance of the three dc-link voltages, a zero sequence current injection method is presented [22,23]. A zero sequence current i_Z is poured into the three-phase inner currents, which is given by:

$$i_Z = \sqrt{2} I_Z \sin(\omega t + \alpha) \tag{32}$$

Note that, as Figure 3b shows, the three input currents for every VIENNA module can be divided into two kinds: one is the line current which flows through the power supply; and the other two currents are phase current circulating only among the three VIENNA modules, which are defined here as inner currents. The zero sequence current injected into the inner currents is served to regulate the power flow among the VIENNA modules with no influence on the line currents.

From Equation (4), the input currents for the first VIENNA converter module after the injection of zero sequence current can be expressed as:

$$\begin{cases} i'_{\mathrm{A1}} = i_{A1} = \sqrt{2} I \sin(\omega t) \\ i'_{\mathrm{B1}} = i_{B1} + i_Z = \sqrt{\frac{2}{3}} I \sin(\omega t - 150^\circ) + i_Z \\ i'_{\mathrm{C1}} = i_{C1} - i_Z = \sqrt{\frac{2}{3}} I \sin(\omega t + 150^\circ) - i_Z \end{cases} \tag{33}$$

Under this circumstance, the dynamics of the dc-link voltage of the first VIENNA module given by Equation (21) can be rewritten as:

$$C \frac{du'_{o1}}{dt} = d_{A1} i'_{\mathrm{A1}} + d_{B1} i'_{\mathrm{B1}} + d_{C1} i'_{\mathrm{C1}} - 2 \frac{u'_{o1}}{R_1} \tag{34}$$

Then, the average value of the dc-link voltage for the first VIENNA module after injection will be changed to become:

$$\overline{u'_{o1}} = \overline{u_{o1}} + I_Z R_1 \times \frac{\sqrt{2}}{4} \times M \times \cos(\alpha + 90^\circ) \tag{35}$$

where $\overline{u_{o1}}$ is the average value before the injection of zero sequence current i_Z.

The dc-link voltages of the other VIENNA rectifiers will experience similar changes after injecting zero sequence current i_Z:

$$\overline{u'_{o2}} = \overline{u_{o2}} + I_Z R_2 \times \frac{\sqrt{2}}{4} \times M \times \cos(\alpha - 150^\circ) \tag{36}$$

$$\overline{u'_{o3}} = \overline{u_{o3}} + I_Z R_3 \times \frac{\sqrt{2}}{4} \times M \times \cos(\alpha - 30^\circ) \tag{37}$$

Figure 7a indicates the control diagram for the voltage balancing control. First, error between the reference voltage $U_O{}^*$ and the three sensed dc-link voltages are regulated through a PI controller, and the three PI controller output signals are then used to generate the reference zero sequence current $i_z{}^*$ with the required amplitude and phase angle. The voltage loop forces the average dc-link voltages of three VIENNA modules to follow $U_O{}^*$ in Figure 6. $\mathrm{Sin}(\omega t + 150^\circ)$ in Figure 7a corresponds to u_{o1}, and if $U_O{}^* > u_{o1}$, then the product of u_{o1} and i_Z forms positive active power.

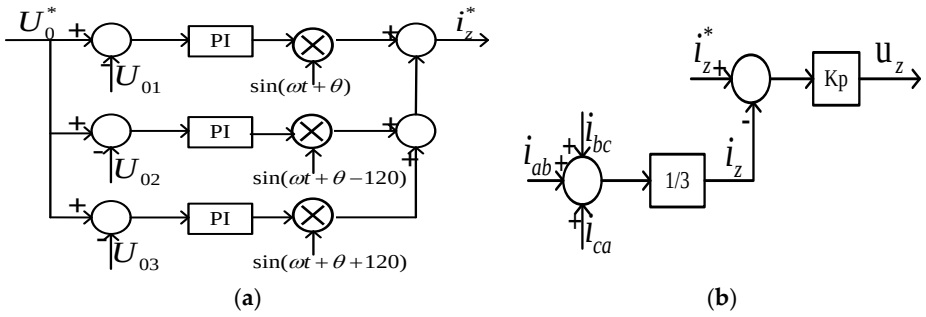

Figure 7. The dc link voltage control. (**a**) zero sequence current generation. (**b**) the zero sequence current following.

Figure 7b displays the zero sequence current control where the inner current loop forces i_Z to follow its command i_z^*.

5.2. Hierarchical Control Strategy

A hierarchical control method is presented to realize the desired power factor, as well as the balanced output dc-link voltages. Figure 8 shows the system overall control. The overall system consists of four parts:

- one-cycle control
- average voltage control
- balanced voltage control
- zero sequence current control

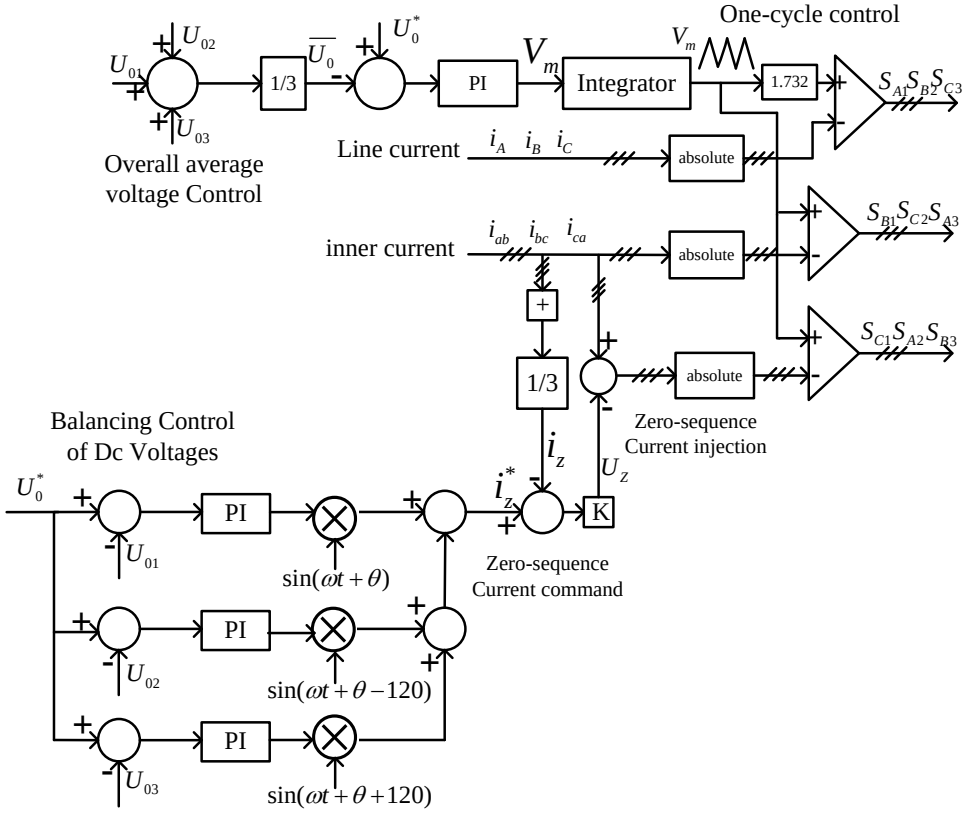

Figure 8. The system overall control.

First, it built the average voltage loop to regulate three dc-link voltages to follow the command voltage $U_0{}^*$. In the voltage balancing control part, as mentioned above, the outer voltage loop generates the reference zero sequence current $i_Z{}^*$ with the required amplitude and phase angle, and the inner current loop forces i_Z to follow its command $i_Z{}^*$.The output of the inner current loop is added to the input of the one circle controller to redistribute the power among the three VIENNA modules, eventually ensuring that the three dc-link voltages of LVC-VC are always kept in balance with the value required by the voltage command $U_0{}^*$, and generating the input current in sinusoidal waveform under unity power factor.

6. Simulation and Experimental Results

Simulation built on Psim has verified the proposed LVC-VC and control strategy under different operating conditions with either balanced loads or unbalanced loads. The detailed parameters for LVC-VC on Psim are shown in Table 3.

Table 3. Simulation Parameters for LVC-VC.

Parameter	Value
Input line-line voltage	6000 V (rms)
Input frequency	50 HZ
dc-link capacitance	4000 μF
dc-link voltage	4800 V
switching frequency	5 KHZ
input inductance	2 mH
Load resistance	100 Ω

Figure 9 shows the currents flowing through different branches. Figure 9a shows the three input line currents which are flowing symmetrically with sinusoidal waveforms. Figure 9b displays the three inner currents flowing through three inductors in Δ connection, as shown in Figure 3. Figure 9c displays the three input currents of the VIENNA rectifier module 1. It can be seen that one of the three is the line current, and the other two are phase currents. The three dc-link voltages are shown in Figure 9d, which are have an equal average value (4800 V) with approximately 40 V fluctuation, so the switch voltage stress is 50 percent of the dc-link voltages, with a value of only 2500 V.

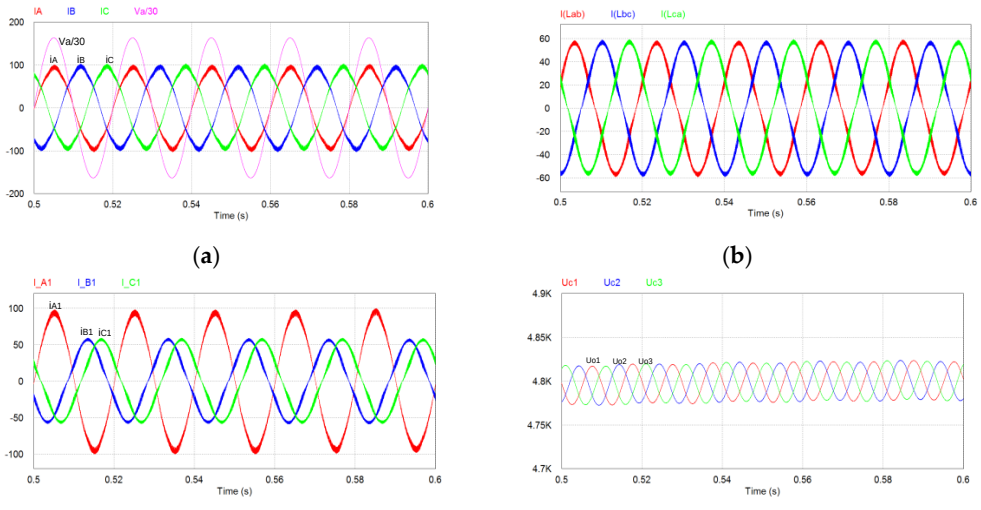

(**a**) (**b**)

(**c**) (**d**)

Figure 9. Simulation waveforms. (**a**) the grid line currents. (**b**) the delta connected inner currents. (**c**) the ac-side currents of the VIENNA rectifier unit 1. (**d**) the dc-link voltages of three VIENNA units.

In Figure 10a, the dc-link voltages are unbalanced when the loads are unbalanced. A balanced recovery transient is shown in Figure 10b, where the LVC-VC initially operates with a balanced load, at $t = 0.5$ s. When the three loads change from $R_1 = R_2 = R_3 = 100\ \Omega$ to $R_1 = 90\ \Omega$, $R_2 = 110\ \Omega$, $R_3 = 100\ \Omega$, the dc-link voltages then became severely imbalanced. However, regulated by one circle control based controller with the aforementioned voltage balancing control scheme, the three dc-link voltages converge to the same average value with an approximate transient time of 1 s.

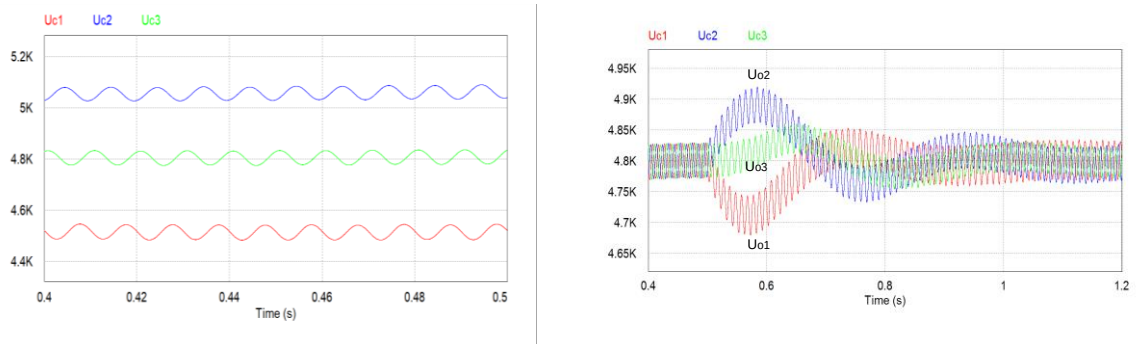

(**a**) (**b**)

Figure 10. The dc-link voltages simulation waveforms in unbalanced loads. (**a**) no zero sequence current injection. (**b**) after the zero sequence current injection.

All the experimental waveforms were taken in an experimental development platform shown in Figure 11, where the controller is the DSP. Experimental waveforms were obtained from the 300VA downscaled model in Table 4. Voltage and current waveforms correspond to those in Figure 12. These figures indicate: (1) the line-line voltage between two VIENNA units (see Figure 12a); (2) the power factor correction (see Figure 12b); (3) the ac-side currents and the dc-link voltage of VIENNA rectifier unit 1 (see Figure 12c); (4) the three dc-link voltages in balanced loads (see Figure 12d); and (5) three dc-link voltages of the proposed converter under three unbalanced dc loads, shown in Figure 12e. The purpose of Figure 12e is to verify the validity of the balancing control scheme through injection of some zero sequence current. Figure 12e shows three dc-link voltages of the proposed converter under three unbalanced dc loads. At first, the three dc-link voltages are unbalanced, but after injecting a zero sequence current, the three dc-link voltages gradually become balanced.

Table 4. Experimental Parameters for LVC-VC.

Parameter	Value
Input line-line voltage	60 V (rms)
Input frequency	50 HZ
dc-link capacitance	500 μF
dc-link voltage	70 V
switching frequency	5 KHZ
input inductance	1.7 mH
Load resistance	50 Ω

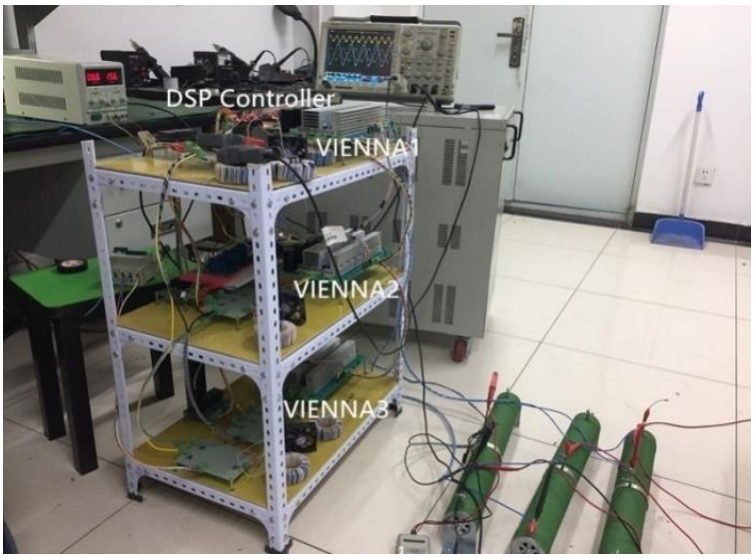

Figure 11. Experimental platform.

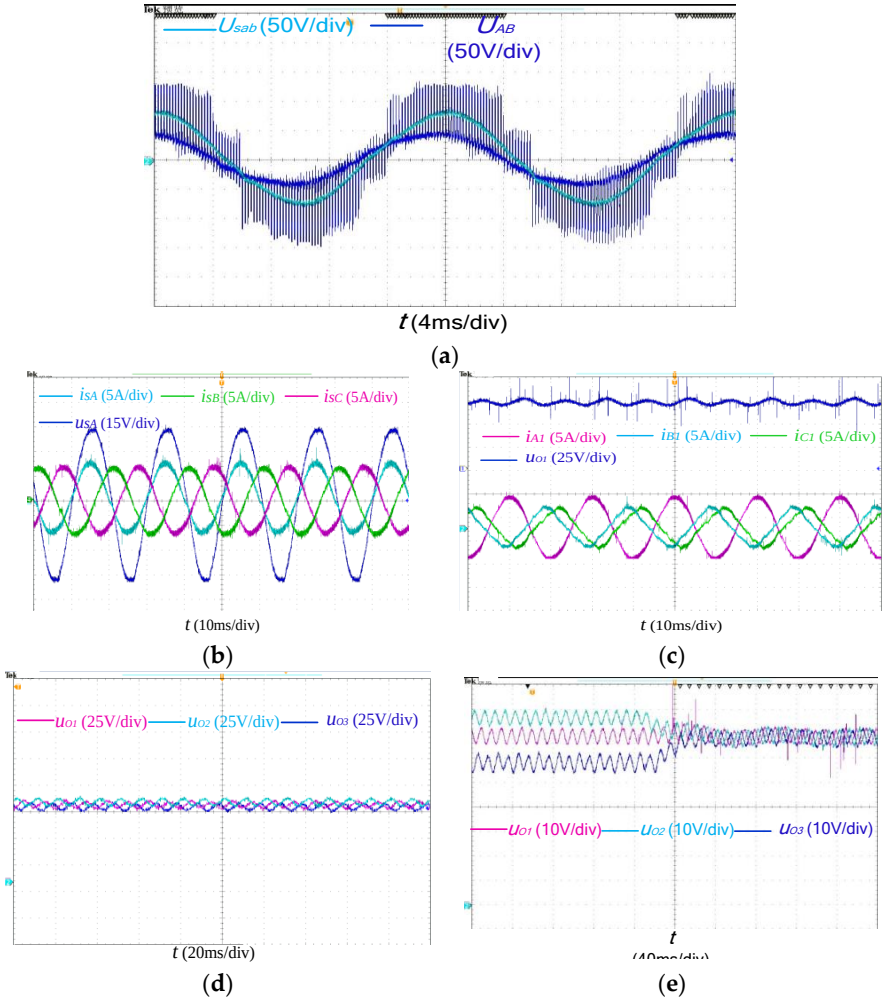

Figure 12. Experimental waveforms. (**a**) the line-line voltage between two VIENNA units. (**b**) the grid line currents. (**c**) the ac-side currents and the dc-link voltage of VIENNA unit 1. (**d**) three dc-link voltages in balanced loads. (**e**) three dc-link voltages in unbalanced loads.

7. Conclusions

In this paper, a new three-phase rectifier based on triple line-voltage cascaded VIENNA converters has been proposed. Comprehensive analysis of the proposed converter is presented. In contrast with traditional three-phase cascaded H-bridge converters, in the proposed new multilevel converters, the switch voltage stress is reduced, and fewer switches and dc capacitors are required under similar operating conditions. The modeling and control of this topology are introduced. The power factor correction of the proposed converter is realized by employing the traditional one-cycle control strategy. To suppress the unbalanced dc-link voltages, a controlled zero sequence current is injected into the inner currents. Simulations and experimental results proved the availability and validity of the new multilevel converters. As a result, the proposed LVC-VC is appropriate as the rectifier in the Medium-Voltage AC Drive.

Author Contributions: J.Z. and C.W. designed the research; H.C. collected and compiled the data and literature; J.L. finished the experiment.

Acknowledgments: This work was supported by the National Natural Science Foundation of China under Grant No. 51577187, and the Fundamental Research Funds for the Central Universities (2015QJ11).

Conflicts of Interest: The authors declare no conflict of interest.

References

1. Rodriguez, J.; Lai, J.S.; Peng, F.Z. Multilevel inverters: A survey of topologies, controls, and applications. *IEEE Trans. Ind. Electron.* **2002**, *49*, 724–738. [CrossRef]
2. Akagi, H. Classification, terminology, and application of the modular multilevel cascade converter (MMCC). *IEEE Trans. Power Electron.* **2011**, *11*, 3119–3130. [CrossRef]
3. Malinowski, M.; Gopakumar, K.; Rodriguez, J.; Perez, M.A. A survey on cascaded multilevel inverters. *IEEE Trans. Ind. Electron.* **2010**, *7*, 2197–2206. [CrossRef]
4. Meireles, E.C.; Antonio, P.M. Control of cascaded H-bridge inverters using an FPGA-based platform. In Proceedings of the International Conference on Power Engineering Energy and Electrical Drives, Torremolinos, Malaga, Spain, 11–13 May 2011.
5. Hagiwara, M.; Nishimura, K.; Akagi, H. A medium-voltage motor drive with a modular multilevel PWM inverter. *IEEE Trans. Power Electron.* **2010**, *7*, 1786–1799. [CrossRef]
6. Akagi, H.; Inoue, S. Medium-voltage power conversion systems in the next generation. In Proceedings of the Power Electronics and Motion Control Conference, Shanghai, China, 14–16 August 2006; pp. 23–30.
7. Wang, D.; Yang, J.W.; Zhu, C. A transformerless medium voltage multiphase motor drive system. *Energies* **2016**, *9*, 1–14.
8. Wang, K.; Zheng, Z.; Li, Y. A Novel transformerless cascaded multilevel converter topology. *Trans. China Electrotech. Soc.* **2011**, *26*, 1–6.
9. Wang, C.; Zhuang, Y.; Jiao, J. Topologies and control strategies of cascaded bridgeless multilevel rectifiers. *IEEE J. Emerg. Sel. Topics Power Electron.* **2017**, *5*, 432–444. [CrossRef]
10. Babaei, E. A cascade multilevel converter topology with reduced number of switches. *IEEE Trans. Power Electron.* **2008**, *6*, 2657–2664. [CrossRef]
11. Wen, J.; Smedley, K.M. Synthesis of multilevel converters based on single and/or three-phase converter building blocks. *IEEE Trans.Power Electron.* **2008**, *3*, 1247–1256. [CrossRef]
12. Wen, J.; Zhou, L.; Smedley, K. Reactive power compensation and harmonics elimination at medium-voltage using hexagram converter. In Proceedings of the Energy Conversion Congress and Exposition (ECCE), Atlanta, GA, USA, 12–16 September 2010; pp. 136–144.
13. Fabricio, E.; Jacobina, C. Multilevel converter based on cascaded three-leg converters with reduced voltage and current. *IEEE Trans. Ind. Appl.* **2017**, *5*, 4682–4694. [CrossRef]
14. Jacobina, C.; Fabricio, E.; Menezes, A. Shunt compensator based on three-phase interconnected converters. In Proceedings of the Energy Conversion Congress and Exposition (ECCE), Denver, CO, USA, 15–19 September 2013; pp. 5222–5228.

15. Lu, Z.; Zhao, L. Research on cascaded three-phase-bridge multilevel converter based on CPS-PWM. *IET Power Electron.* **2013**, *6*, 1088–1099. [CrossRef]
16. Xia, C.; Zhou, F.; Wang, Z. Equivalent switch circuit model and proportional resonant control for triple line-voltage cascaded voltage-source converter. *IEEE Trans. Power Electron.* **2013**, *28*, 2389–2401. [CrossRef]
17. Xia, C.; Wang, Z.; He, X. An improved control strategy of triple line-voltage cascaded voltage source converter based on proportional-resonant controller. *IEEE Trans. Ind. Appl.* **2013**, *7*, 2894–2902. [CrossRef]
18. Dieckerhoff, S.; Bernet, S.; Krug, D. Power loss-oriented evaluation of high voltage IGBTs and multilevel converters in transformerless traction applications. *IEEE Trans. Power Electron.* **2005**, *7*, 1328–1332. [CrossRef]
19. Qiao, C.; Smedley, K. Three-phase unity power factor star connected switch (VIENNA) Rectifier with Unified Constant-Frequency Integration Control. *IEEE Trans. Power Electron.* **2003**, *18*, 952–957. [CrossRef]
20. Chen, Y.; Smedley, K. Parallel operation of one-cycle controlled three-Phase PFC rectifiers. *IEEE Trans. Ind. Appl.* **2007**, *54*, 3217–3224. [CrossRef]
21. Wei, Z.; Chen, X.; Fan, T. Study and analysis of neutral-point potential and control methods for one-cycle controlled three-phase three-level VIENNA rectifiers. In Proceedings of the CSEE, Beijing, China, 25 May 2013; pp. 29–33.
22. Ding, W.L.; Zhang, C.H.; Gao, F. A zero-sequence component injection modulation method with compensation for current harmonic mitigation of VIENNA rectifier. *IEEE Trans. Power Electron.* **2018**. [CrossRef]
23. Hagiwara, M.; Maeda, R.; Akagi, H. Negative-sequence reactive-power control by a PWM STATCOM based on a modular multilevel cascade converter. In Proceedings of the Energy Conversion Congress and Exposition (ECCE), Phoenix, AZ, USA, 17–22 September 2011; pp. 3728–3735.